Available online at www.ilcpa.pl

International Letters of Chemistry, Physics and Astronomy

10(2) (2013) 137-150 ISSN 2299-3843

Effect Cd Doping on the Structural and Optical Properties of ZnO Thin Films

J. A. Najim, J. M. Rozaiq

Physics Department, College of Science, Anbar University, Anbar, Iraq

E-mail address: Ifaris38@yahoo.com

ABSTRACT

ZnO thin films with Cd/Zn nominal ratios of 0 %, 1 %, 3 %, 5 %, and 7 % and thickness of 0.7 μm were prepared by chemical spray pyrolysis. X-ray diffraction patterns showed that the films have polycrystalline structures and peaks matching the hexagonal ZnO structure. Crystallite sizes ranged from about 35 nm to 87 nm. As the doping concentration increased, full width at half maximum values decreased and crystallite sizes increased. The UV-Vis spectra of the ZnO:Cd films showed high transparency in the visible region. The optical band gap of the ZnO:Cd films decreased from 3.255 eV to 3.17 eV with increasing Cd doping concentration. The transition type was direct, thereby allowing transition. The ZnO:Cd thin films were annealed at 400 °C, and annealing treatment showed improvements in the properties of the derived films.

***Keywords*:** ZnO thin films ,semiconductor doping,optical properties, structure properties.

1. INTRODUCTION

Transparent conducting oxide (TCO) thin films have received a great deal of attention because of their wide applications in optoelectronic devices [1]. TCOs have high thermal stability and low cost [2-5]. ZnO, one of the most promising TCOs currently available, has high transparency in the visible region of the electromagnetic spectrum to oxygen vacancies. It has band gap of approximately 3.2-3.3 eV and does not contain any element that is hazardous to the environment [5,6].

ZnO, a member of the II-VI group of semiconductors, has been applied in light-emitting diodes, laser emission, window materials, solar cells, gas sensors [7-12,35], and surface acoustic wave devices. Impurity doping is necessary for the successful manipulation of the physical properties of ZnO doped with Cd [13,14]. The structural properties of the compound are affected by changes in composition because ZnO has hexagonal structure and CdO has a cubic structure.

The band gap varies with the doping concentration of the films from about 3.3 eV of ZnO [25-27] to about 2.2 eV of CdO [25-27]. Incorporation of Cd into ZnO is very useful for the fabrication of ZnO/ZnCdO heterojunction and super lattice structures [1].

ZnO:Cd thin films can be prepared using different methods, such as electro-deposition, pulsed laser deposition, molecular beam epitaxy, sol-gel process, and spray pyrolysis [14-23]. The spray pyrolysis method is used for preparing large numbers of pure and doped thin films because the method is simple, inexpensive, and easy to apply for growing uniform films and allows the coating of large areas [1,24]. This work aims to study the effects of doping concentration and annealing on the structural, morphological, and optical properties of Cd-doped ZnO thin films.

2. EXPERIMENTAL

ZnO:Cd thin films were prepared in a spray pyrolysis system. The molar ratio was 0.2 M, the Cd/Zn nominal ratios were 0 %, 1 %, 3 %, 5 %, and 7 % and the film thickness on the glass substrates was 0.7 μm. The substrate temperature was fixed at 370 °C and controlled within +5 °C using a digital thermo coupler (chromel-alumel). The solution flow rate was 2 mL/min and the gas pressure was about 5×10^4 N / m^2.

Prior to deposition, glass substrates were cleaned with acetone, ethanol, and distilled water. The X-ray diffraction (XRD) spectra of the films were obtained to verify their crystal structure using a (Cu-K_α) radiation with λ = 0.154 nm. Optical transmission data were obtained using an UV-Vis double beam spectrometer at wavelengths ranging from 200 nm to 900 nm. Optical microscopy, atomic force microscopy (AFM) and scanning electron microscopy (SEM) were employed to observe the surface morphology of the films. The prepared films were annealed at 400 °C for 1 h in air.

3. REASULTS AND DISCUSSION

Fig. 1 (a) shows the XRD patterns of ZnO:Cd films with different doping concentrations. The films are polycrystalline, with a hexagonal wurtzite type crystal structure and preferred orientation in the (100) direction. The (100) peak appeared with maximum intensity, and other peaks at (002), (101) and (110) were observed as is expected of the hexagonal ZnO structure [28].

This finding indicates that the films have strongly preferred a-axis orientation, which may be attributed to minimization of the crystal surface free energy [1]. Doping with Cd led to changes in the XRD peak intensities. At low doping concentrations, the increase in peak intensity is attributed to the formation of new nucleating centers caused by a decrease in the nucleation energy barrier. However, at higher doping concentrations, the decrease in peak intensity is attributed to the increased saturation of new nucleating centers [1,22].

The lattice constants (unit cell parameters of ZnO thin films) a and c were calculated from the XRD patterns as 3.27 and 5.242 Å, respectively, both of which are in good agreement with the bulk values [3,4,12,15,28-30]. The XRD patterns of the ZnO:Cd thin films annealed at 400 °C are shown in Fig. 1(b).

The intensity of the peaks increased with annealing treatment, leading to improvements in the crystallinity of the derived films. This result may be due to the energy provided by the annealing temperature to the film atoms.

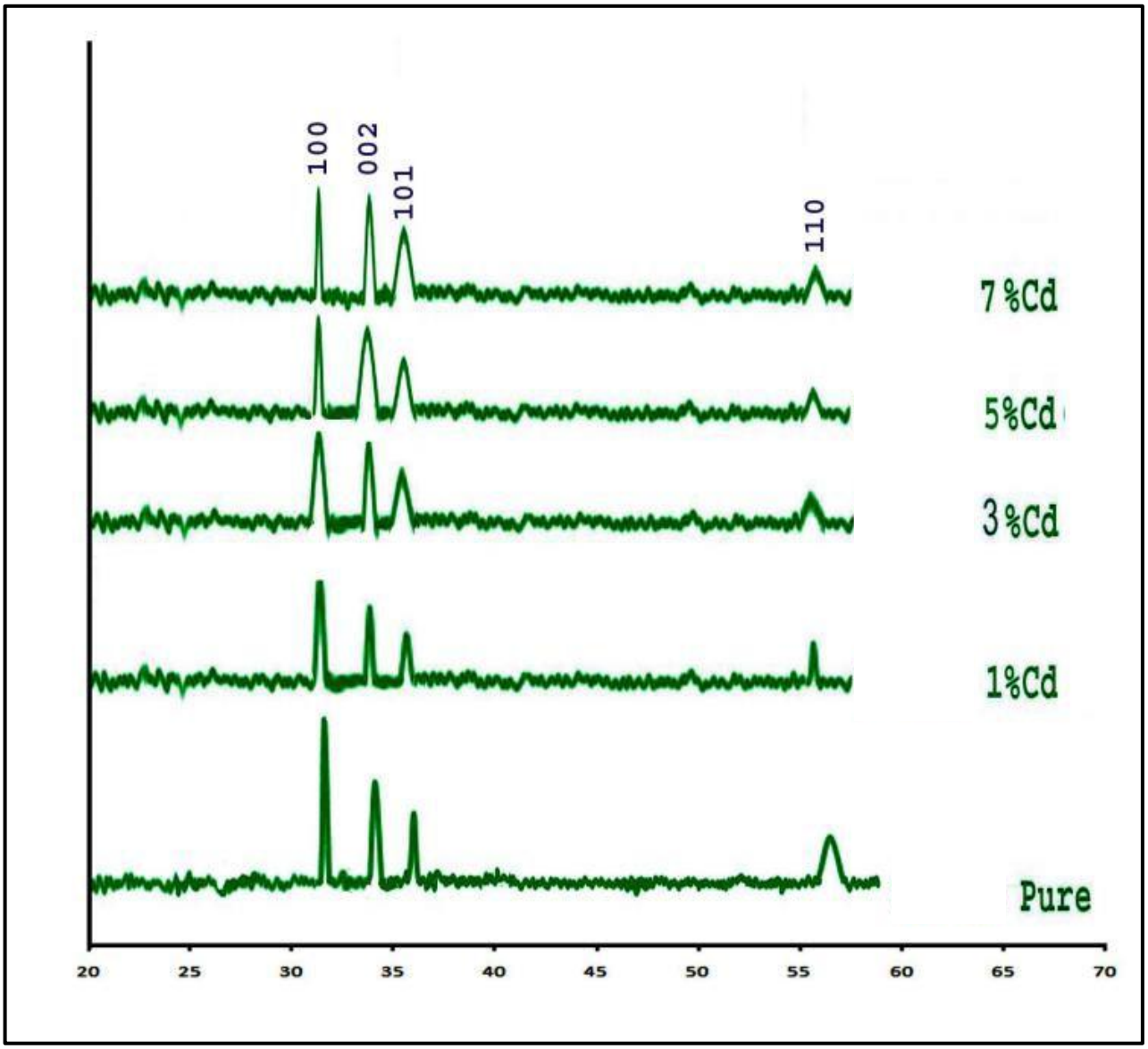

(a)

Fig. 1 (a). XRD patterns for the annealed ZnO deposited thin films with different content of Cd.

Such energy enhances the mobility of atoms to decrease the number of defects in the films. Improvements in crystallinity may also be due to relaxation of the existing residual compressive stresses between ZnO and the glass substrate [31,32].

The crystallite size was estimated using Scherrer's formula [33]:

$$D = k\lambda / \beta \cos \beta \ldots (1)$$

where D represents the diameter of the crystallites, λ is the X-ray wavelength, β is the full width at half maximum and K is a constant nearly equal to one. The values of D are shown in Table 1.

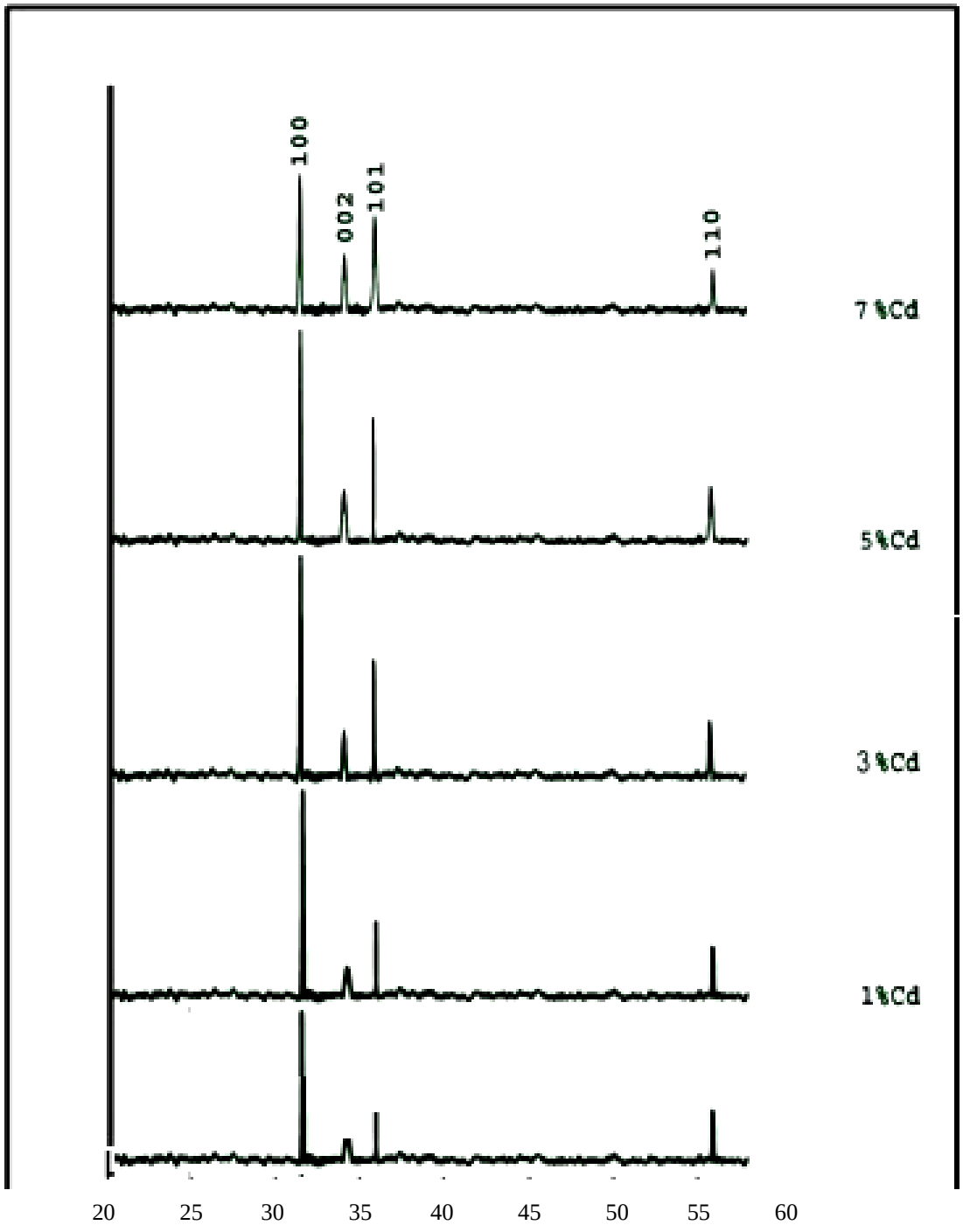

(b)

Fig. 1 (b). XRD patterns for the annealed ZnO deposited thin films with different content of Cd.

Table 1. Crystallite sizes of ZnO:Cd thin films.

Concentration		Pure	1 %	3 %	5 %	7 %
Crystallite Size (nm)	Before annealing	42.1	35	70	35	87
	After annealing at 400 °C	93.2	104.9	119	84.2	70

Variations in crystallite size with doping concentration may be explained in a number of ways: First, the decrease in crystallite size could be due to an increase in number of Cd atoms, which would exert drag forces on boundary motion and grain growth. Second, the increase in the number of dopant atoms may lead to increased numbers of point defects, which would give rise to higher grain boundary mobility and grain growth rates [1,34].

Figs. 2 and 3 show microscope images of the as-grown ZnO: Cd thin films. Grain growth was clearly detected, and surfaces of the films were smooth and homogeneous. The grains grew to large sizes when the films were annealed at 400 °C, and each grain was composed of several crystallites [1,28]. Inter-grain connections also increased with annealing temperature.

Fig. 4 shows SEM images of ZnO films with various particle sizes. The surface morphology of the films varies with the oxidation temperature. The sample oxidized at a temperature of 400 °C shows a smooth surface with uniform particles compared with the as-grown sample. The grain size increased as a function of annealing temperature, as confirmed by the XRD spectra. We believe that due to the strain of the surface as function of annealing temperatures. As-grown film particles are under compressive strain, and strain relaxation increases with temperature [1, 31]. No impurities or structural defects, such as vacancies and zinc interstitials, were observed.

Fig. 5 shows AFM images of the ZnO:Cd films before and after annealing. Fig. 5a shows an image of the as-grown sample with a smooth surface topography and root-mean-square (RMS) of 6.35 nm (10 μm × 10 μm scan area) and average roughness of 4.82 nm. This observation indicates better film quality and a surface with pyramidal shape were distributed over the entire surface. Fig. 5b shows the same thin film after annealing at 400 °C; here, the RMS was 17.4 nm and the roughness was 12.3 nm. This result also agrees with XRD findings [32].

The increase in pyramidal shape indicates that the increase in the surface roughness affects the surface characterization of the films and leads to changes in the optical, electronic, and vibrational transitions of the material.

The increase in roughness of the film surface indicates the possibility of using the synthesized films as anti-reflection-coatings, which reduce light reflection. Surface roughness is an important parameter for enhancing the photo conversion process of some devices, such as solar cells and photo detectors [32].

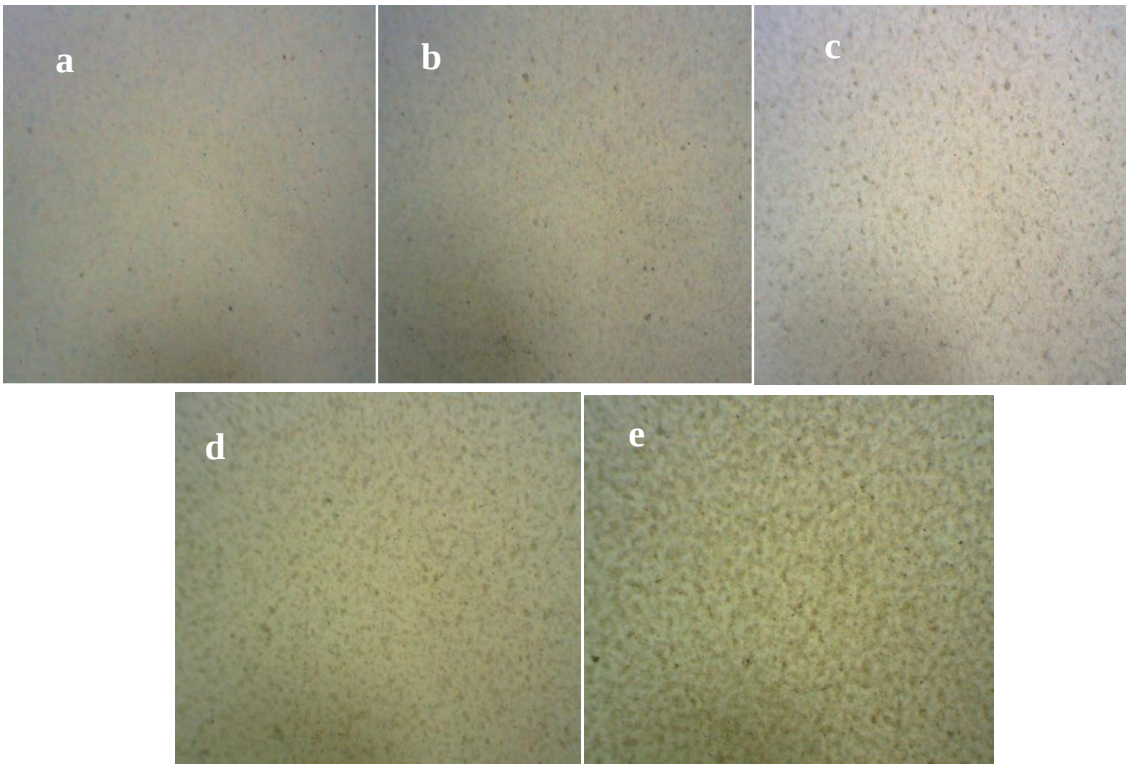

Fig. 2. Photo microscopic images before annealing. (a) Pure ZnO, (b) ZnO doped with 1 % Cd, (c) ZnO doped with 3 % Cd, (d) ZnO doped with 5 % Cd and (e) ZnO doped with 7 % Cd.

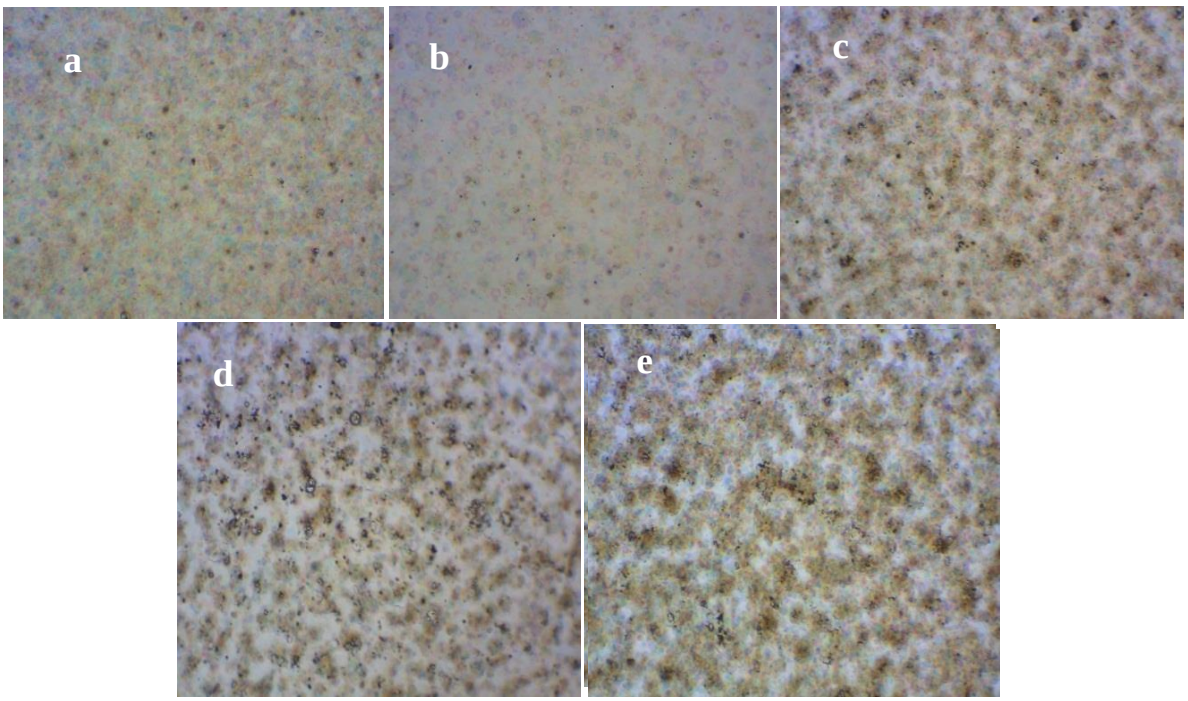

Fig. 3. Photo microscopic images after annealing. (a) Pure ZnO, (b) ZnO doped with 1 % Cd, (c) ZnO doped with 3 % Cd, (d) ZnO doped with 5 % Cd and (e) ZnO doped with 7 % Cd.

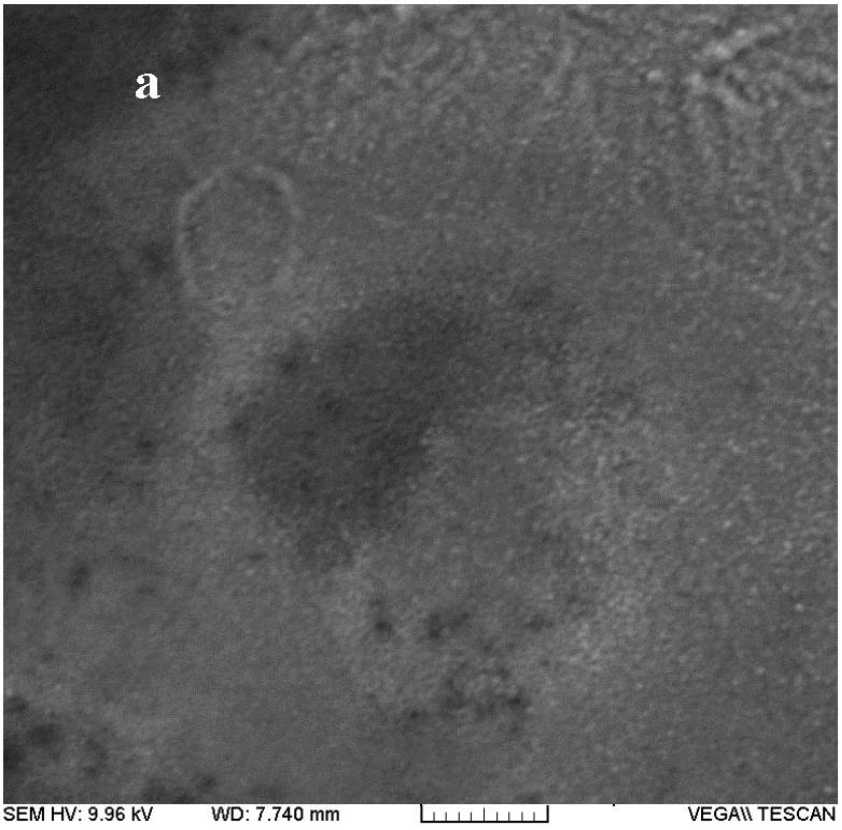

Fig. 4. SEM micrograph for for ZnO:cd a) before annealing b) after annealing.

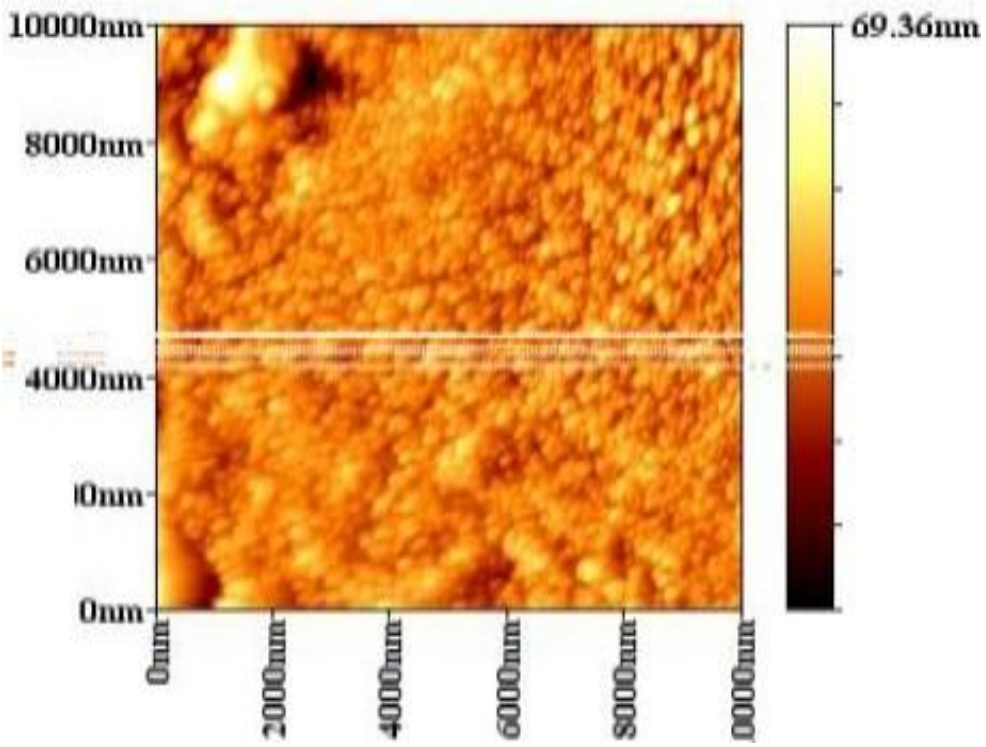

Sa(Roughness Average) 4.8 2 [nm]
Sq(Root Mean Square) 6.35 [nm]

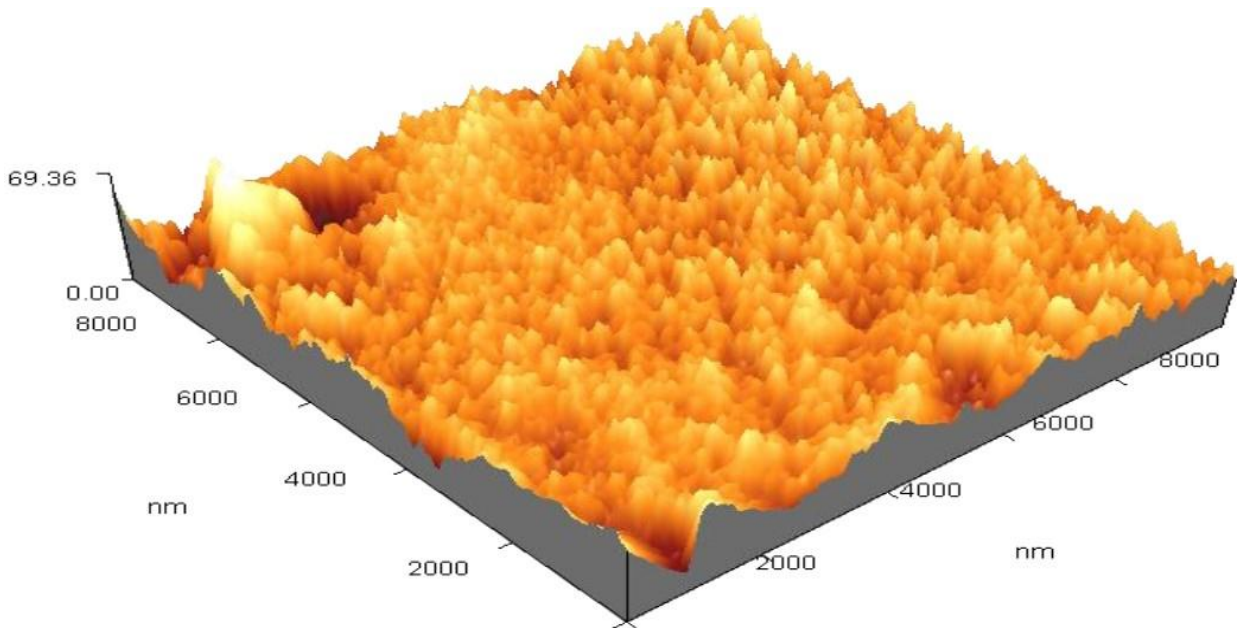

Fig. 5. AFM micrograph for ZnO:Cd a) before annealing b) after annealing.

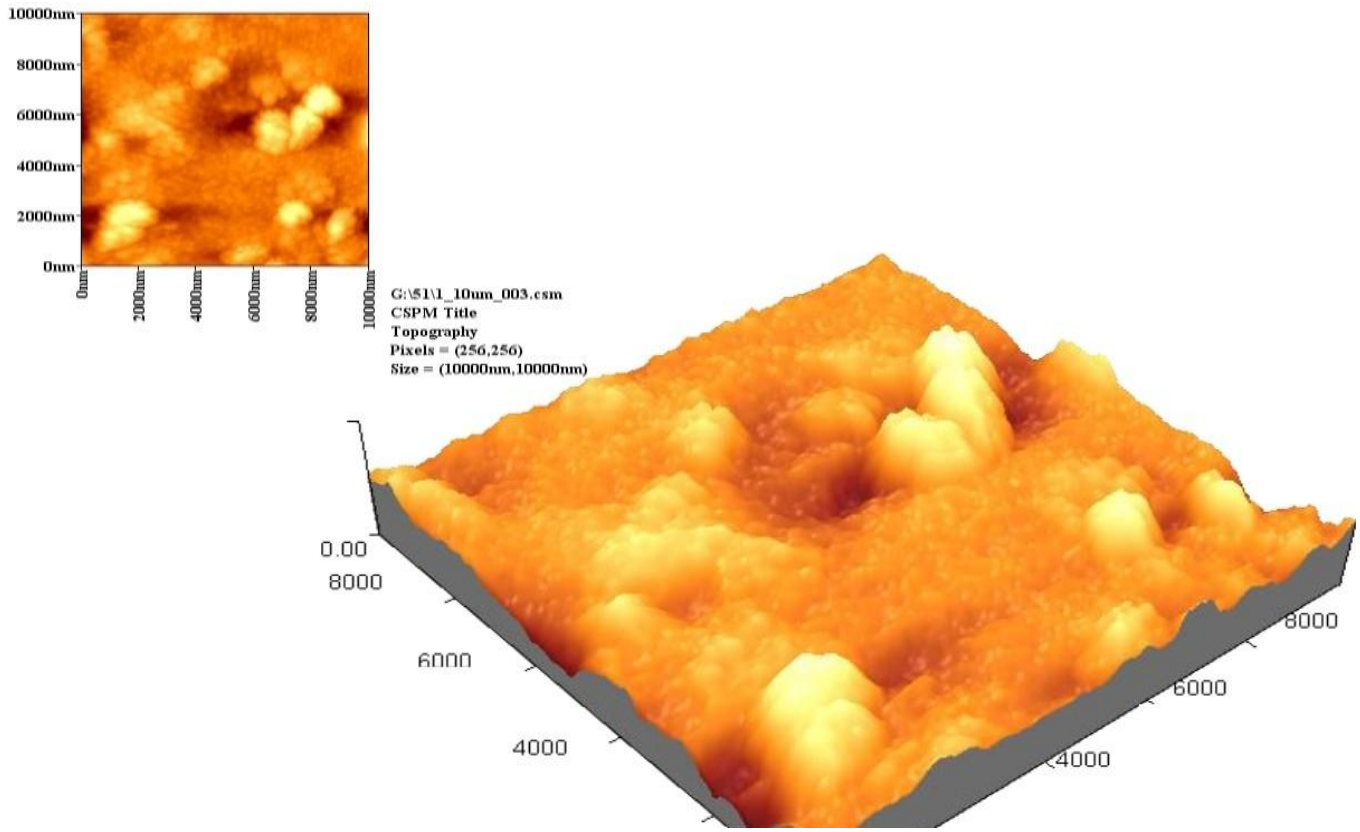

Fig. 5 (continue). AFM micrograph for ZnO:Cd a) before annealing b) after annealing.

Fig. 6 (a) shows the optical transmission of the ZnO:Cd films. The optical transmission of the films decreased with doping concentration, which gives a satisfactory optical window for optoelectronic applications [3]. The decrease in transmittance at higher doping concentrations may be attributed to the increased scattering of photons by crystal defects created by doping.

The free carrier absorption of photons may also contribute to the observed reduction in the optical transmission of heavily doped films and thin film interference effects [3,29]. The optical transmission spectra of the ZnO:Cd films annealed at 400 °C are shown in Fig. 6 (b), where a red shift in the transmission threshold and a reduction of the average transmission may be observed [5].

The decrease in transmittance is due to the increase in scattering centers or defects formed after annealing [31].

The absorption coefficient (α) was calculated by:

$$\alpha = 2.303\ A / t \quad \ldots\ldots\ldots \quad (2)$$

The type of transition was directly allowed transition because the dependence of α on the photon energy (hν) was found to obey the following relationship:

$$\alpha h\nu = A'(h\nu - Eg)^{1/2} \quad \ldots.(3)$$

where A' is a constant and Eg is the band gap. A plot of $(\alpha h\nu)^2$ versus hν shows the optical band gap of films with direct transition, as shown in Fig. 7.

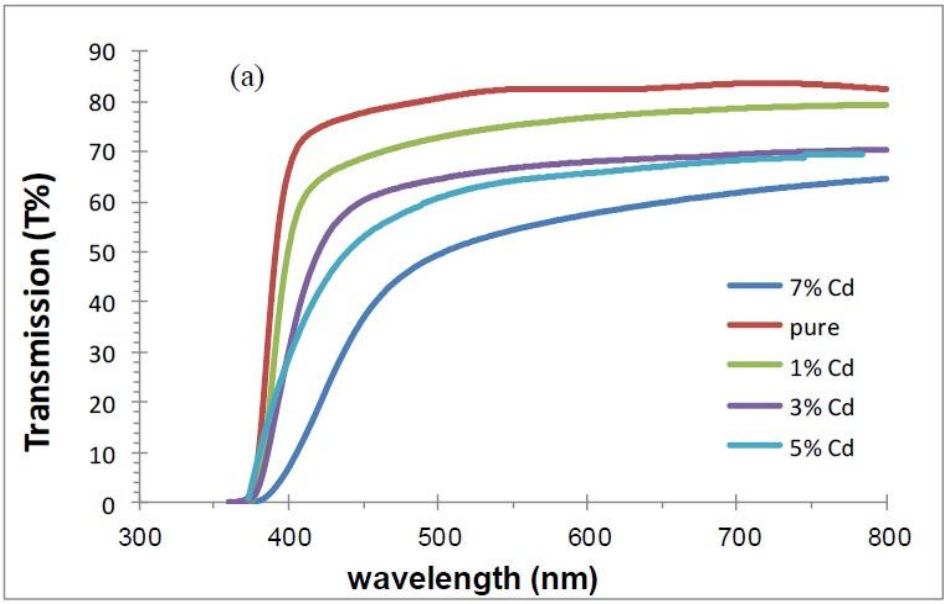

Fig. 6 (a). Optical transmission of ZnO:Cd.

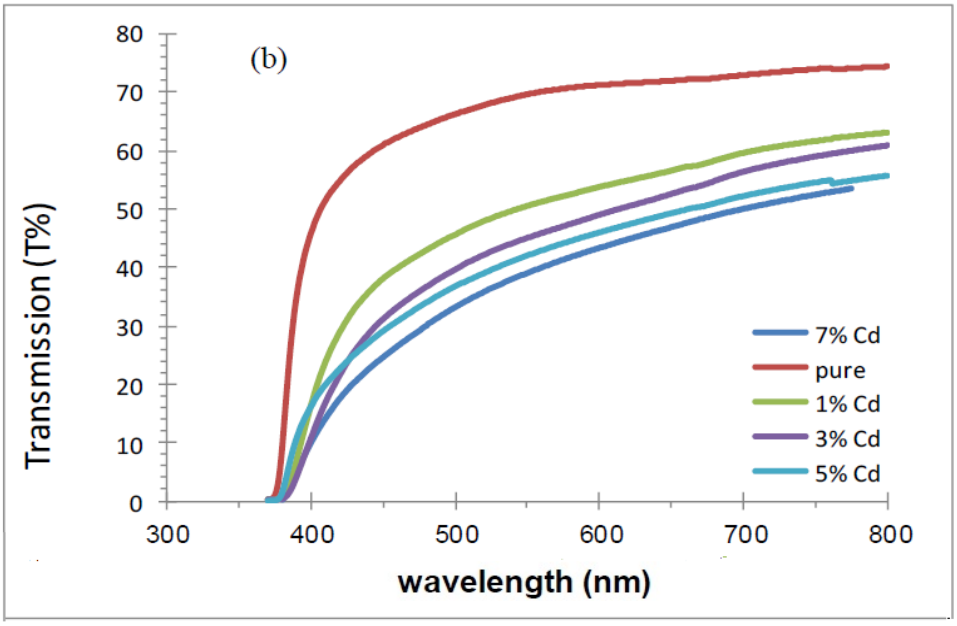

Fig. 6 (b). optical transmission of the annealed ZnO:Cd thin films.

The values of the band-gap energy of the ZnO films with different doping concentrations are shown Fig. 7 (a). The Cd content increased as the optical band gap decreased from 3.255 eV to 3.17 eV. This result agrees with other works [8,29]. The absorption edge exhibited a red shift as the Cd doping concentration increased [1,14,34]. The presence of Cd impurities in the ZnO structure induced the formation of new recombination centers with lower emission energies [1,8]. The reduction in band gap with increasing Cd content is attributed to hybridization of the electronic states of Zn-4s and Cd-5s.

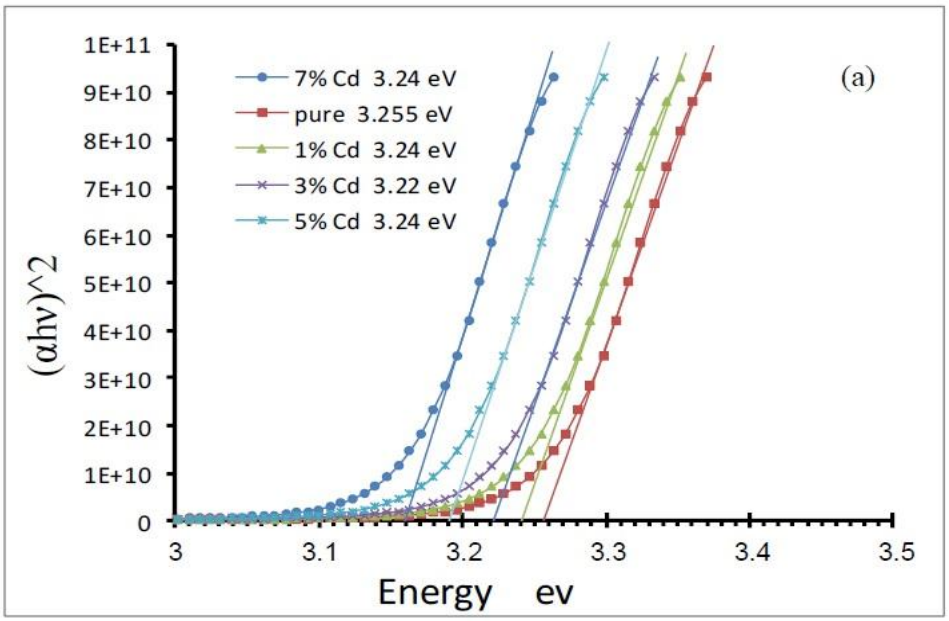

Fig. 7 (a). Optical energy gap of ZnO: Cd thin films.

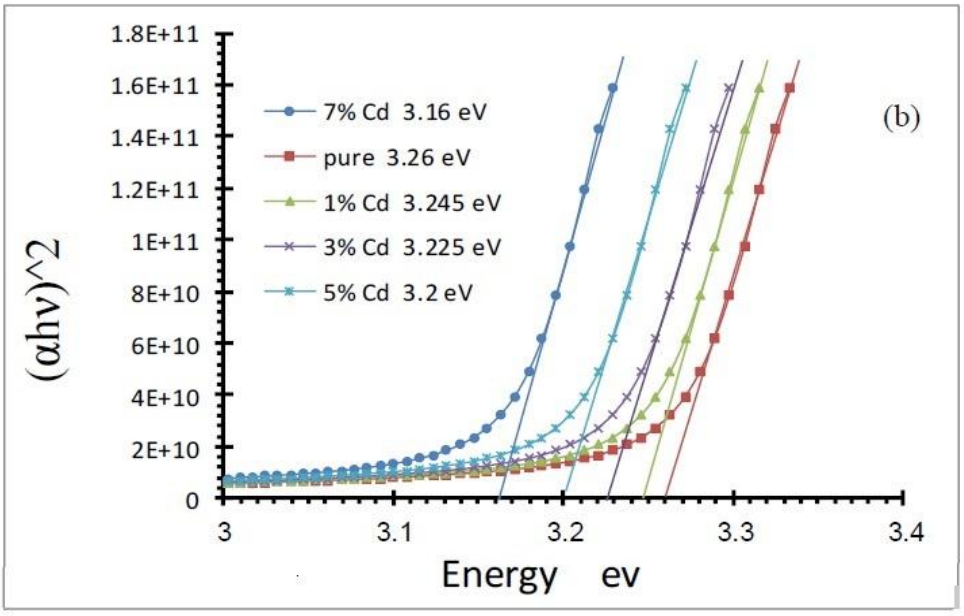

Fig. 7 (b). Optical energy gap of the annealed ZnO: Cd thin films.

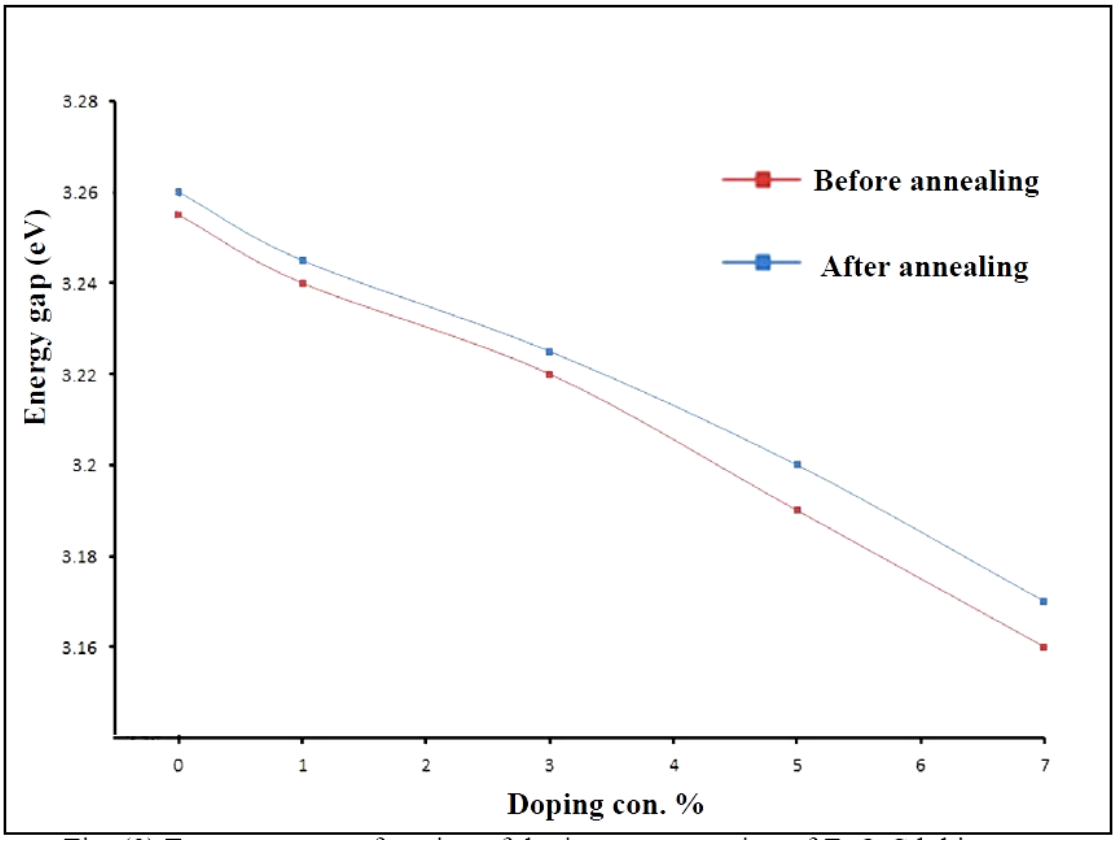

Fig. 8. The value of the optical energy gap before and after annealing for all the samples.

Fig. 7b shows that the optical absorption edge shifted to short wavelengths when the ZnO:Cd thin films were annealed at 400 °C. This blue shift could be attributed due to the motion of Fermi level owing to increase in the charge carrier concentration as annealing temperature or attributed to the decrease in shallow- level trap concentration near the conduction band [1,5,32]. The increase in band gap with thermal annealing of the as-grown and annealed ZnO:Cd thin films as a function of concentration is shown in Fig. 8. The trend observed may be attributed to the fact that the grains grow larger as the annealing temperature increases, which leads to increased point defect concentrations that may also give rise to higher grain boundary mobility and grain growth rate.

4. CONCLUSION

XRD analysis showed that polycrystalline film grain sizes first increased and then decreased as the number of dopant atoms increased. Grains grew to larger sizes when annealed at 400 °C due to enhancements in atomic diffusion. The films showed preferential orientation in the direction of the a-axis. The absorption edge showed a red shift, and the optical band gap of the thin films decreased as the Cd doping increased but increased with annealing at 400 °C. The optical transmission of the films decreased with increasing doping concentration, which provides a satisfactory optical window for optoelectronic applications.

REFERENCES

[1] G. Li, X. Zhu, X. Tang, W. Song, Z. Yang, J. Dai, Y. Sun, X. Pan, S. Dai, *Journal of Alloys and Compounds* 509 (2011) 4816-4823.

[2] A. A. Yousif, A. J. Haidar, N. F. Hbubi, *Int. J. Nanoelctronics and Materials* 5 (2012) 47-55.

[3] C.M. Muiva, Y. S. Sathiaraj, K. Maabong, *Ceramic International* 37 (2011) 555-560.

[4] J. Naya, S. Kimura, S. Nazaki, H. One, K. Uchida, *Superlattices and Microstructures* 42 (2007) 438-443.

[5] G. Santana, A. Morales, O. Vigil, L. Vallant, F. Cruz, G. Contreras, *Thin Solid Films* 373 (2000) 235-238.

[6] Y. Yang, H. Chen, B. Zhao, X. Bao, *Journal of Crystal Growth* 263 (2004) 447-453.

[7] R. Ayouchi, D. Leinen, F. Martin Gapas, E. Dalchiele, J. R. Barrado, *Thin Solid Films* 426 (2003) 68-77.

[8] F. Yakuphanoglu, S. Ilican, M. Caglar, Y. Caglar, *Superlattice and Microstures* 47 (2010) 732-743 .

[9] A. E. Suliman, Y. Tang, *L. Solar Energ. Materials and Solar cells* 91 (2007) 1658-1662 .

[10] S. D. Shine, G. E. Patil, D. D. Kajale, V. B. Gaikwad, G. H. Jain, *Jornal of Alloys and Componds* 528 (2012) 109-114 .

[11] F. Paraguay D., M. Miki-Yoshida, J. Morales, J. Solis, W. Estrada L., *Thin Solid Films* 373 (2000) 137-140 .

[12] R.Y. Hong, J. Z. Qion, J. X. Cao, *Powder Technology* 163 (2006) 160-168.

[13] D. Zaouk, Y. Zaatar, R. Asmar Jabbour, *Microelectronics Journa* l37 (2006) 1276-1279.

[14] M. Tortosa, M. B. Mair, *Journal of Crystal Growth* 304 (2007) 97-102.

[15] H. S. Kang, S. H. Lim, J. W. Kim, H. W. Chany, G. H. Kim, S. Y. Lee, Y. Li , J. Lee, J. K. Lee, M. A. Nastusi, S. A. Crooker, Q. X. Jia, *Jornal of Crystal Growth* 287 (2006) 70-73 .

[16] K. J. Chen, T. H. Fang. F.Y. Hung, L. W. Ji, S. J. Chang, S. J. Young, Y. J. Hsiao, *Applied Surface Science* 254 (2008) 5791-5795 .

[17] K. Sakurai, T. Takagi, T. Kubo, D. Kajita, T. Tanabe, H. Takasu, S. Fujita, Sh. Fujita, *Journal of Crystal Growth* 237-239 (2002) 514-517 .

[18] A. Erol, S. Okur, B. Comba, O. Mermer, C. Arikan, *Sensors and Actuators B: Chemical* 145(1) (2010) 174-180.

[19] D. Zhao, Y. Liu, D. Shen. Y. Lu, J. Zhang , X. Fan, *Journal of Crystal Growth* 234 (2002) 427-430 .

[20] B. L. Zhu, C. S. Xie, D. W. Zeng, W. L. Song, A. H. Wang, *Materials Chemistry and Physics* 89 (2005) 148-153 .

[21] Z. Ben Achour, T. Ktar, B. O. Touagyar, B. Bessais, J. Ben Brahim, *Sensors and Actuators A* 134 (2007) 447-451 .

[22] C. Cumus, O. M. Ozkendir, H. Kavak, Y. Ufuk tepe, *Journal of Opticalectronics and Advanced Material* 8 (2006) 299-303.

[23] F. Paraguay, W. Estrada, D. R. Acosta, E. Andrade, M. Miki-Yoshida, *Thin Solid Films* 350 (1999) 192-202 .

[24] S. Vijayalashmi, S. Venkataraj, R. Jayavel, *J. Phys. D: Appl. Phys.* 41 (2008) 245403 (7PP).

[25] G. Santana, A. Morales, O. Vigil, L. Vallant, F. Cruz, G. Contreras, *Thin Solid Films* 373 (2000) 235-238 .

[26] D. Zhang, F. Zeng, *J. Mate. Sci.* 47 (2012) 2155-2161 .

[27] J. Z. Liu, P. X. Yan, G. H. Yue, J. B. Chang, R. F. Zhuo, D. M. Qu, *Matterials Letters* 60 (2006) 3122-3125 .

[28] P. Mitra, J. Khan, *Material Chemistry and Physics* 98 (2006) 279-284.

[29] P. Prepelita, R. Medianu, B. Sbarcea, F. Garoi, M. Filipescu, *Applied Science* 256 (2010) 1807-1811.

[30] Z. Bi. Ju, L. Jian-She, Z. Lei, J. Qing, *Chin. Phy. Lett.* 28 (2011) 016801.

[31] A. Arora, Anil Arora, P. J. George, V. K. Dwivedi, V. Gupta, *Sensors and Transducers Journal* 117 (2010) 92-98 .

[32] Asmiet Ramizy, Z. Hassan, Khalid Omar, *MBE. Journal of Nanopartical Research* 13 (2011) 7139-7148.

[33] S. Cimitan, S. Albonetti, L. Forni, F. Peri, D. Lazzari, *Journal of Colloid and Interface Science* 329 (2009) 73-80 .

[34] S. Vijayalakshmi, S. Venkataraj, R. Jayavel, *J. Phys. D: Appl. Phys*. 41 (2008) 245403.

[35] Saad F. Oboudi, Nadir F. Habubi, Ghuson H. Mohamed, Sami S. Chiad, *International Letters of Chemistry, Physics and Astronomy* 8(1) (2013) 78-86.

(Received 02 June 2013; accepted 06 June 2013)